Collective Directional Transport in Coupled Nonlinear Oscillators without External Bias

Zhigang Zheng,[1] Gang Hu,[2,1] and Bambi Hu[3,4]
[1]Department of Physics, Beijing Normal University, Beijing 100875, China
[2]China Center of Advanced Science and Technology (CCAST), P.O. Box 8730, Beijing 100080, China
[3]Center for Nonlinear Studies and Department of Physics, Hong Kong Baptist University, Hong Kong, China
[4]Department of Physics, University of Houston, Houston, Texas 77204
(Received 25 August 2000)

Directed collective motion in a circular array of unidirectionally coupled oscillators with symmetric potential is obtained numerically in the absence of external bias. This striking feature is interpreted as the effect of the spontaneous breaking of temporal symmetry of the coupling. It is revealed that a proper match of various control parameters is important in generating an optimal coherent global transport. Noise-sustained directed transport is also observed, and the related stochastic resonance in an autonomous system is identified.

DOI: 10.1103/PhysRevLett.86.2273 PACS numbers: 05.45.Xt, 05.45.Pq, 05.60.Cd

Cooperative phenomena of interacting oscillator systems have been extensively investigated in relating to a variety of behaviors such as synchronizations, clustering [1], collective transport, and nonlinear waves [2]. Recently, a subject of significance is the directional transport behavior in the presence of an external potential field without bias. For instance, directed transport of oscillators can be induced by a ratchet potential with broken spatiotemporal symmetry. This has been investigated in recent decades on various context organisms [3,4]. Till now, however, very little attention has been paid to the collective transport dynamics of spatiotemporal systems in this aspect. So far as we know, a collective directed motion can appear in a system consisting of a large number of coupled subsystems only in the presence of external drift (i.e., bias). Thus, it is of great theoretical interest to ask whether we can find spatiotemporal systems which manifest global transport in the absence of external bias, and if the answer is positive, a further important topic is to reveal the mechanism underlying such a striking feature. Practically, this study may open a new direction to understand the rich macroscopic transportation behaviors of chainlike objects under symmetric global field in various disciplines of natural science (in particular, in biological systems) from the dynamics of microscopic subunits and their interactions. We show in this Letter that the directed motion can be induced by a unidirectional internal coupling and symmetric field in the absence of an external bias. We interpret this as the effect of the coupling-induced ac force, which breaks the temporal symmetry. Currents both along and reversal to the coupling direction are found and analyzed. The pinning and depinning transition of the coupled array is revealed by varying a control parameter. Noise-sustained directed transport and the associated stochastic resonance is observed.

We start with a typical model of broad interest: the one-dimensional lattice of N oscillators with nearest-neighbor couplings:

$$\dot{\mathbf{X}}_i = \mathbf{f}_i(\mathbf{X}_i) + (\varepsilon + r)\mathbf{g}(\mathbf{X}_{i+1} - \mathbf{X}_i) - (\varepsilon - r)\mathbf{g}(\mathbf{X}_i - \mathbf{X}_{i-1}), \qquad (1)$$

where $i = 1, 2, \ldots, N$ and ε and r denote the diffusive and the gradient couplings, respectively. $\dot{\mathbf{X}}_i = \mathbf{f}(\mathbf{X}_i)$ describes the nonlinear dynamics of a single oscillator, with $\mathbf{X}_i = [x_i(1), x_i(2), \ldots, x_i(n)]$ being the phase-space variables. $\mathbf{g}(\mathbf{x})$ represents the coupling function. System (1) is a generalization of diffusively coupled oscillators, which has been extensively studied [5]. For $n = 1$, if $f(x) = -d\sin x$ and $g(x) = x - a$, Eq. (1) gives the dynamics of the array of N coupled overdamped pendula: $\dot{x}_i = -d\sin x_i + (\varepsilon + r)(x_{i+1} - x_i - a) - (\varepsilon - r)(x_i - x_{i-1} - a)$, where d is the height of the potential barrier and $a = 2\pi\delta$ is the static spring length ($0 \le \delta \le 1$ is the frustration, measuring the mismatch between the potential period 2π and the static length a). When $r = 0$, this system goes back to the famous Frenkel-Kontorova (FK) model in the overdamped case, which has been adopted as a representative model in various contexts [6]. Therefore this is a generalization of the FK model. In this Letter, we study the case of unidirectional coupling, $r = \varepsilon = 1/2$. Unidirectional coupling plays a significant role in understanding numerous behaviors in information transmissions in neuron systems [7] and traffic flow [8]; moreover, it can be easily realized in electric circuits [9] and coupled Josephson junctions [4]. By adopting the periodic boundary condition, the equation of motion can be written as

$$\dot{x}_i = -d\sin x_i + (x_{i+1} - x_i - a), \quad x_{i+N} = x_i + Na. \qquad (2)$$

$Na = 2\pi M$, where M is an integer indicating the number of circles of the whole chain (each site has 2π length). A collective current can be defined as $J(t) = \frac{1}{N}\sum_{i=1}^{N}\dot{x}_i(t)$. It is emphasized that the parameter a in Eq. (2) is not a bias; it determines only the relative distance between two neighbor sites, not the direction of the global motion. When $d = 0$, it is easily found that (2) has a stationary solution $x_i = \alpha + ia$ with α being arbitrary, and no directed collective motion can be observed, i.e., $J(t) = 0$.

For both $d \to 0$ (strong coupling) and $d \gg 1$ (weak coupling) limits, we have $J(t) = 0$. As a finite external field is applied, i.e., $0 < d \propto O(1)$, it is interesting whether there is a net directed current. In Fig. 1, evolutions of $x_i(t)$ and $J_i(t) = \dot{x}_i(t)$ at $d = 0.05$, 1.2, and 3.77 are presented for $a = \pi/5$. For small d, a slow directed motion of the array can be found [see Figs. 1(a) and 1(b)]. Because of the strong coupling, the motion is nearly uniform. When d is large, a typical stick-slip feature is observed [see Figs. 1(c)–1(f)]. It is interesting to notice that for moderate d, as shown in Figs. 1(c) and 1(d), the array moves with a larger velocity; i.e., there exists an optimal d (coupling) that produces a maximum transport current. In Figs. 2(a) and 2(b), the average current $J = \lim_{T\to\infty} \frac{1}{T} \int_0^T J(t)$ varying with d and δ are computed. It is intriguing that for each $\delta \neq 0, 1$, there is an optimal d_0 that possesses a maximum current. For any δ there is a critical d value d_c, over which a pinning transition occurs, i.e., $J = \dot{x}_i = 0$ for $d > d_c$. For small $d \to 0$ and for $d \to d_c$, $J \to 0$ via the scaling laws $J \propto d^2$ and $J \propto (d_c - d)^{1/2}$, respectively. The frustration δ plays a significant role in determining the transport properties. It can be seen from the J vs δ relation given in Fig. 2(b) that all curves are antisymmetric about $\delta = 1/2$. For $\delta > 1/2$, current reversal $J < 0$, i.e., the directed transport occurs against the coupling direction, can be observed in a large region. The reversed current can also be found around $\delta = 1/2$ for moderate d [see Fig. 2(a) for $\delta = 15/32$]. For small couplings (large d), the array is pinned for some values of δ. It is interesting to note that an optimal frustration exists also for the system to have the best efficiency of directed transport.

For both small and large d ($d > d_c$), further numerical and theoretical analyses can be undertaken. Let us first consider the case of $d \ll 1$. For $d = 0$, we have $J = 0$, and then $x^0_{i+1} = x^0_i + a$ and $x^0_i - x^0_j = (i - j)a$. For $d \ll 1$, the array moves uniformly with a small velocity; therefore, by using the adiabatic approximation [neglecting $\dot{x}_i$ in Eqs. (2), which will be consistently shown to be of d^2 order], one obtains $x_{i+1} \approx x_i + a + d\sin x_i$; i.e., the spatial configuration is sinusoidally modulated by the amplitude d. By summing over Eqs. (2), one has $J(t) = -\beta d$, where $\beta = \frac{1}{N}\sum_{i=1}^N \sin x_i$. Thus an important task is to work out this summation. To the first-order approximation, one has $\beta \approx \frac{1}{N}\sum_{i=1}^N \sin x^0_i + \frac{d}{N}\sum_{i=1}^N \cos x^0_i \times \sum_{j=1}^{i-1} \sin x^0_j$. Obviously $\beta_0 = \frac{1}{N}\sum_{i=1}^N \sin x^0_i = 0$; then one has $\beta \approx \frac{d}{2N}\{\sum_{i,j}\sin(x^0_i + x^0_j) - \sum_{i,j}\sin[(i-j)a]\} = -\frac{d}{2N}\sum_{i,j}\sin[(i-j)a]$, where the summations are for $j < i$. For $a = 0$ and 2π ($\delta = 0, 1$), $\beta = 0$, thus $J = 0$. For $a \neq 0$ or 2π, one gets

$$\beta \approx -\frac{d}{4}\left[\tan\left(\frac{a}{2}\right)\right]^{-1} \qquad (a \neq 0, 2\pi). \qquad (3)$$

Therefore we obtain the average net current for small d:

$$J(d,\delta) = C(d,\delta)d^2, \qquad \lim_{d\to 0} C(d,\delta) = C(\delta) = [4\tan(\pi\delta)]^{-1} \qquad (\delta \neq 0, 1). \qquad (4)$$

This formula, which is exact for $d \to 0$, explains the scaling relation $J \propto d^2$ for $d \ll 1$. To make a comparison with numerical results, in Fig. 2(c) we plot the function $C(\delta)$ in (4) by a dashed line. The diamond line corresponds to results of direct simulation of Eqs. (2) for $d = 0.01 \ll 1$. The agreement is perfect. Moreover, it can be found from (4) that $J(d,\delta)$ is antisymmetric with respect to δ about $\delta = 1/2$, $C(d, 1/2 + \delta) = -C(d, 1/2 - \delta)$.

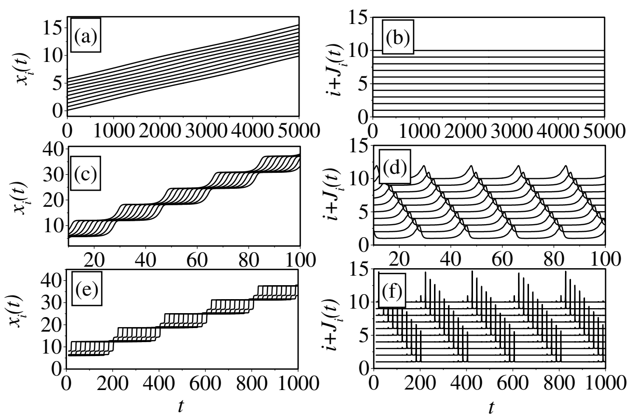

FIG. 1. The evolution of the positions $x_i(t)$ and velocities $J_i(t)$ of particles. $a = \pi/5$ ($\delta = 0.1$). (a),(b) $d = 0.05$, (c),(d) $d = 1.2$, and (e),(f) $d = 3.77$. For simulations, the number of the sites is chosen as such that the rational number δ takes the form $\delta = M/N$ with M and N being two irreducible integers, and this role is applied for all the following figures.

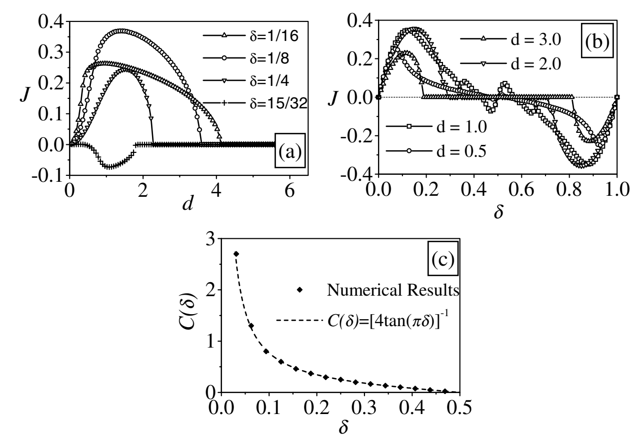

FIG. 2. (a) J varying with d for $\delta = 1/16$, 1/8, 1/4, and 15/32; (b) J vs δ for $d = 0.5$, 1.0, 2.0, and 3.0; (c) a comparison between numerical results of Eq. (2) for $d = 0.01 \ll 1$ (diamonds) and theoretical function $C(\delta)$ in Eq. (4) (dashed line). Perfect agreement is shown.

This interprets the symmetry property and the current reversal behavior in Fig. 2(b) for small d.

It is instructive to explore the origin of this coupling-induced directed current. For $d \neq 0$, the structure of the array is modulated by the sinusoidal field. Microscopically, this leads to a nonuniform interaction for each oscillator from other sites. One may define an effective force on the ith oscillator as $F^i_{\mathrm{eff}}(t) = x_{i+1} - x_i - a$. In Fig. 3(a), the effective force on the first oscillator for $d = 1.0$ and $\delta = 1/32$ is plotted. This force is time periodic, $F^i_{\mathrm{eff}}(t + T) = F^i_{\mathrm{eff}}(t)$. Effective forces acting on other oscillators possess the same form but with different phases. Significantly, this periodic force is neither symmetric nor antisymmetric with respect to t, i.e., $F^i_{\mathrm{eff}}(-t) \neq F^i_{\mathrm{eff}}(t)$, and $F^i_{\mathrm{eff}}(t \pm \frac{T}{2}) \neq -F^i_{\mathrm{eff}}(t)$. Moreover, within one period $\int_T^{t+T} F^i_{\mathrm{eff}}(t)\,dt = 0$, as shown from positive and negative parts labeled in Fig. 3(a). Thus, these forces have zero mean for both time and space, i.e., $\frac{1}{T}\int_0^T F^i_{\mathrm{eff}}(t)\,dt = 0$ and $\sum_{i=1}^N F^i_{\mathrm{eff}}(t) = 0$, but are temporally asymmetric in each time period. It is just this temporal asymmetry that leads to a short but strong drive in one direction and a long but weak force in the other direction, resulting in a preferred direction of transport. One may apply this force to drive a response oscillator: $\dot{x}_r = -d_r \sin x_r + F^i_{\mathrm{eff}}(t)$. The evolution of the response system for $d_r = d = 1$ is plotted in Fig. 3(b). A directional stick-slip motion is reproduced. Flach *et al.* [10] considered the motion of a particle in a 1D periodic potential under the influence of an ac force. If the ac force breaks the time symmetry, they claimed that a directed current can exist. Our result supports this proposition. An essentially significant point here is that in the present case, the asymmetric periodic force is self-organized among the oscillators by the internal coupling, not artificially applied.

Let us turn to the second point, the behavior around d_c. When $d > d_c$, $\dot{x}_i = 0$, then the stationary state of (2) is the sine-circle map:

$$x_{i+1} = x_i + 2\pi\delta + d\sin x_i\,, \qquad (5)$$

which has been well studied as a paradigmatic model for phase locking, quasiperiodicity, and chaos. In Fig. 4(a),

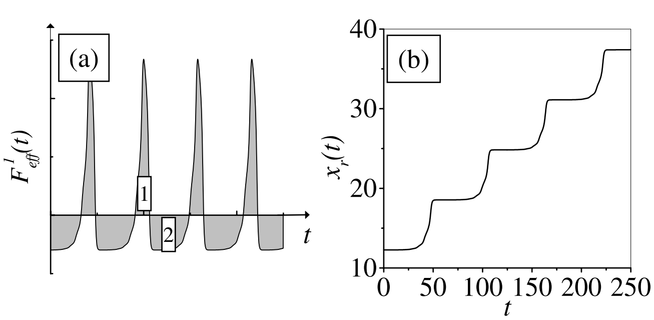

FIG. 3. (a) $F^1_{\mathrm{eff}}(t)$ for $d = 1.0$ and $\delta = 1/32$; (b) the evolution of the response system for $d_r = d$. Directed stick-slip motion is produced.

we plot the bifurcation diagram of map (5) with 2π modulo for $\delta = 1/32$. It can be found that a *crisis,* i.e., a sudden expansion of size of the chaotic attractor, occurs at $d_{cr} = 4.37$. The J vs d relation is also plotted in Fig. 4(a) by a diamond line at $\delta = 1/32$ for system (2). A striking result is that the J vs d curve turns to $J = 0$ at $d_c \approx d_{cr}$, i.e., just at the d value for the crisis. In Fig. 4(b), we plot both d_{cr} and d_c vs δ, and we have $d_{cr} \approx d_c$ in a large range of δ. This identity is very similar to Aubry's commensurate-incommensurate phase transition in the FK model [11], where the pinning-depinning transition corresponds to the destruction of the last KAM torus in the standard map (area-preserving). For the present case, the pinning transition is shown to correspond to crisis in the circle map (dissipative).

A heuristic understanding of the mechanism for this correspondence can be given as follows. Crisis is known to happen when an unstable periodic orbit collides with the boundary of the chaotic attractor [12]. In Fig. 4(a) the unstable period-1 orbit (UPO-1) of (5) $x^u = 2\pi - \sin^{-1}(2\pi\delta/d)$ is given by a dashed line. Obviously, crisis occurs as the UPO-1 collides with the boundary of the chaotic attractor. To find the relation between crisis and the pinning transition, in Fig. 4(c) we plot the pinning-state configuration of system (2) with 2π modulo for $d = 4.4 > d_c(d_{cr})$. The state of Fig. 4(c) is an unstable period-N state of the circle map (5), embedded in the chaotic state after the crisis (not before the crisis), and this state is also a stable stationary state of Eq. (2). We also give the UPO-1 of (5) in Fig. 4(c) by a solid line. It can

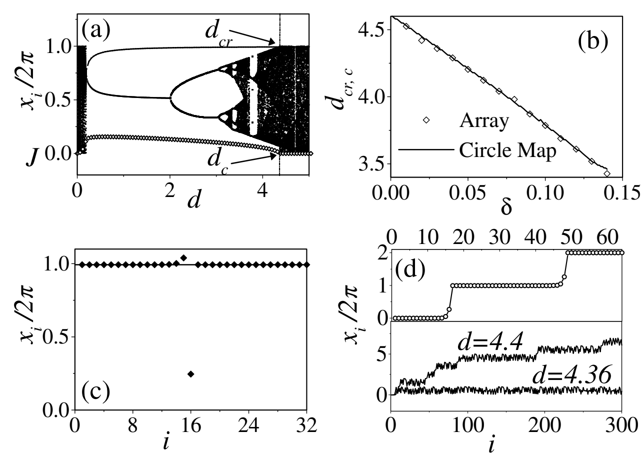

FIG. 4. (a) The bifurcation diagram of the circle map for $\delta = 1/32$. The dashed line denotes the UPO-1 of the circle map, and the diamond line represents J against d. The identity between d_{cr} for the crisis of the circle map and d_c for the pinning transition of Eqs. (2) is apparent. (b) Comparison between d_c and d_{cr} vs δ. (c) The pinning state profile (modulo 2π) of the array for $d = 4.4 > d_c$ and $\delta = 1/32$ (diamond), and the solid line is the corresponding UPO-1. (d) Upper: the pinning state of the array for $d = 4.4$, $\delta = 1/32$ (no 2π modulo); lower: the iterations of the circle map for $d = 4.36 < d_c$ and $4.4 > d_c$. Phase delocalization occurs at d_c.

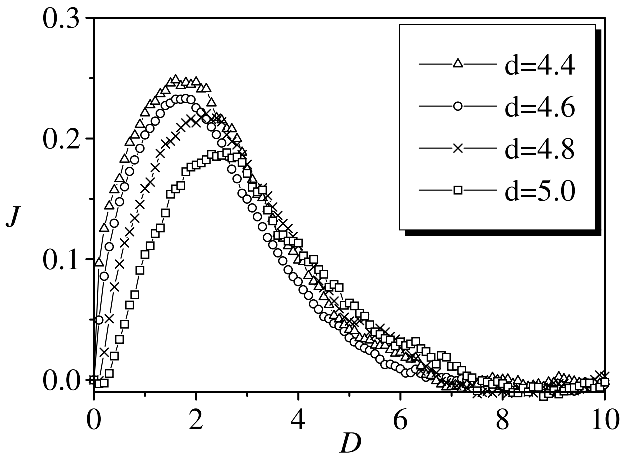

FIG. 5. The stochastic-resonance-like relation between J and the noise intensity D for $d = 4.4$, 4.6, 4.8, and 5.0.

be seen that the basic state of the pinning state is just the UPO-1, with a few deviating spatial "defects." These defects, in fact, are just kinks, as shown in the upper frame of Fig. 4(d) (no 2π modulo). These kinks are absolutely necessary for the basic UPO-1 orbit to fit the boundary conditions of Eqs. (2). For the circle map, crisis in fact implies a delocalization of x_i, i.e., chaos occurs in a larger region (see lower figure, the line $d = 4.4$), leading to a wide chance of pattern selection. This delocalization produces slips for Eq. (5) and can fit the spatial kinks of the pinning state of (2) [see Fig. 4(d) upper frame]. When $d < d_c(d_{cr})$, the orbit x_i of Eq. (5) is localized [see the line $d = 4.36$ of the lower figure in 4(d)]; thus the kink configuration of (2) can never be achieved in this regime by the iterations in space only. This results in the temporal instability of the pinning state and consequently a macroscopic directed motion of the array.

Finally, let us consider the noise effect. Here we simply apply the spatially uncorrelated Gaussian thermal noise: $\langle \xi_i(t) \rangle = 0, \langle \xi_i(t)\xi_j(t') \rangle = D\delta_{i,j}\delta(t - t')$, where D is the noise intensity. Noise can play an important role in the vicinity of the pinning point, because noise can effectively decrease the height of the potential. With a collaboration between noise and the coupling, the disordered energy can be translated into the ordered directed motion. In Fig. 5, we exhibit the relation between J and D for $\delta = 1/32$ at $d = 4.4$, 4.6, 4.8, and $5.0 > d_c = 4.37$. Without noise, these d's lie in the pinning region of $J = 0$. Resonancelike behavior is clearly shown when noise is applied [13]. For small noise, the pinning mechanism dominates and J is very small; for large noise, disorder becomes overwhelming, the directed transport is gradually destructed, and J is small, too. An optimal noise can produce the largest directed transport current. In this case, we find stochastic resonance without external signal and bias, caused by the interplay of the symmetric nonlinear field, one-way coupling, and noise.

In the study of the ratchet problem, one finds that a particle can manifest directional motion under asymmetric potential (which does not offer bias along any direction) together with symmetric nonequilibrium forcing (including noise). Here we show that a coupled system can manifest directional motion under symmetric potential if the coupling is asymmetric (which does not either offer bias along any direction); the directional motion of the 1D chain can be along or reversal to the coupling direction. This new feature may open a new direction to study the collective motion of spatially extended objects, which popularly exist in nature, in particular, in biological systems.

This work is supported by National Natural Science Foundation of China, the Special Funds for Major State Basic Research Projects, and the Foundation for University Key Teacher by the Ministry of Education. B. H. is supported by the Hong Kong Research Grant Council (RGC) and by the Hong Kong Baptist University Faculty Research Grant (FRG).

[1] Y. Kuramoto, *Chemical Oscillations, Waves and Turbulence* (Springer-Verlag, Berlin, 1984).
[2] *Physics of Sliding Friction,* edited by B. N. J. Persson and E. Tosatti (Kluwer Academic Publishers, The Netherlands, 1996).
[3] F. Jülicher *et al.,* Rev. Mod. Phys. **69**, 1269 (1997).
[4] E. Trías *et al.,* Phys. Rev. E **61**, 2257 (2000).
[5] L. Kocarev and U. Parlitz, Phys. Rev. Lett. **76**, 1816 (1996); J. Yang *et al.,* Phys. Rev. Lett. **80**, 496 (1998).
[6] J. Frenkel and T. Kontorova, Phys. Z. Sowjetunion **13**, 1 (1938); Z. Zheng *et al.,* Phys. Rev. B **58**, 5453 (1998).
[7] L. O. Chua *et al.,* IEEE Trans. Circuits Syst. II **35**, 1257 (1988).
[8] M. Bando *et al.,* Phys. Rev. E **51**, 1035 (1995).
[9] M. A. Matías *et al.,* Phys. Rev. Lett. **81**, 4124 (1998).
[10] S. Flach *et al.,* Phys. Rev. Lett. **84**, 2358 (2000).
[11] S. Aubry, Phys. Rep. **103**, 12 (1984).
[12] C. Grebogi, E. Ott, and J. A. Yorke, Phys. Rev. Lett. **48**, 1507 (1982); B. L. Hao, *Elementary Symbolic Dynamics and Chaos in Dissipative Systems* (World Scientific, Singapore, 1989).
[13] L. Gammaitoni *et al.,* Rev. Mod. Phys. **70**, 223 (1998).